J Fluoresc (2014) 24:389–396
DOI 10.1007/s10895-013-1303-x

ORIGINAL PAPER

Fluorescence Properties and Electrochemical Behavior of Some Schiff Bases Derived from N-Aminopyrimidine

Mehmet Gulcan · Ümit Doğru · Gülsiye Öztürk · Abdulkadir Levent · Esvet Akbaş

Received: 28 July 2013 / Accepted: 11 September 2013 / Published online: 21 September 2013

Abstract A series of Schiff bases ($\mathbf{L_1}$, $\mathbf{L_2}$ and $\mathbf{L_3}$) were prepared by refluxing aromatic aldehydes with N-Aminopyrimidine derivatives in methanol and ethanol. The structures of synthesized compounds were characterized by FTIR, ^{1}H NMR, ^{13}C NMR and microanalysis. The electrochemical behaviors of the Schiff base ligands were also discussed. Moreover, the evaluation of absorption and emission properties of the structures were carried out in five different solvents. The products show visible absorption maxima in the range of 304–576 nm, and emission maxima from 636 to 736 nm in all solvents tested.

Keywords Schiff base · fluorescence · N-Aminopyrimidine · electrochemistry

Introduction

Schiff bases are known to be very important class of organic compounds because of their ability to form stable complexes with many different transition metal and rare-earth metal ions in various oxidation states and have the potential to be used in different areas such as catalysis, metallic deactivators, separation processes, electrochemistry, bioinorganic and environmental chemistry [1–5]. Moreover they have increasingly importance in the pharmacological, dye, and plastic industries as well as in the field of liquid crystal technology [6–10]. Pyrimidine is a very important group of compounds that has been extensively studied due to their occurrence in the living systems [11]. Pyrimidines are reported to have broad spectrum of biological activities. Some are endowed with antitumor [12], antiviral [13], anti-inflammatory [14], antipyretic [15], antimicrobial [16], and antifungal [17] properties. During last few decades there has been great interest in the chemistry of transition metals associated with nitrogen, oxygen and sulfur donor ligands, such as five and six membered heterocyclic pyrazoles, pyridazines and pyrimidines [18–21].

In this work the Schiff bases containing a pyrimidine ring were synthesized, characterized and their fluorescence features were determined in different solvents. The compounds were characterized by elemental analysis, FT-IR, ^{1}H and ^{13}C NMR techniques. Moreover, the electrochemical properties of the Schiff bases were investigated.

Results and Discussion

The present work involves the spectroscopic investigation of the Schiff base ligands (L_1, L_2 and L_3) derived from pyrimidine amine. The synthesis protocol of Schiff base ligands has been shown in Fig. 1.

The IR spectra of the L_3 ligand exhibit several bands in the region of 400–4,000 cm^{-1}. The IR spectrum of the ligand showed a ν(C=N) peak at 1,599 cm^{-1} and the absence of ν(C=O) at ~1,680 cm^{-1} and ν(NH$_2$) peaks around 3,250–3,300 cm^{-1} is because of Schiff base condensation. The absorption band at 1,643 cm^{-1} is assigned to benzoyl ν(C=O) moiety. Pyrimidine ring showed characteristic stretching absorption bands at the 3,064 cm^{-1}[22].

M. Gulcan (✉) · E. Akbaş
Department of Chemistry, Faculty of Science,
University of Yuzuncu Yil, 65080 Van, Turkey
e-mail: mehmetgulcan65@gmail.com

Ü. Doğru · G. Öztürk (✉)
Department of Chemistry, Faculty of Science,
University of Dokuz Eylül, 35160 Tınaztepe, Izmir, Turkey
e-mail: gulsiyeozturk@yahoo.com

A. Levent
Health Services Vocational College, Batman University,
72100 Batman, Turkey

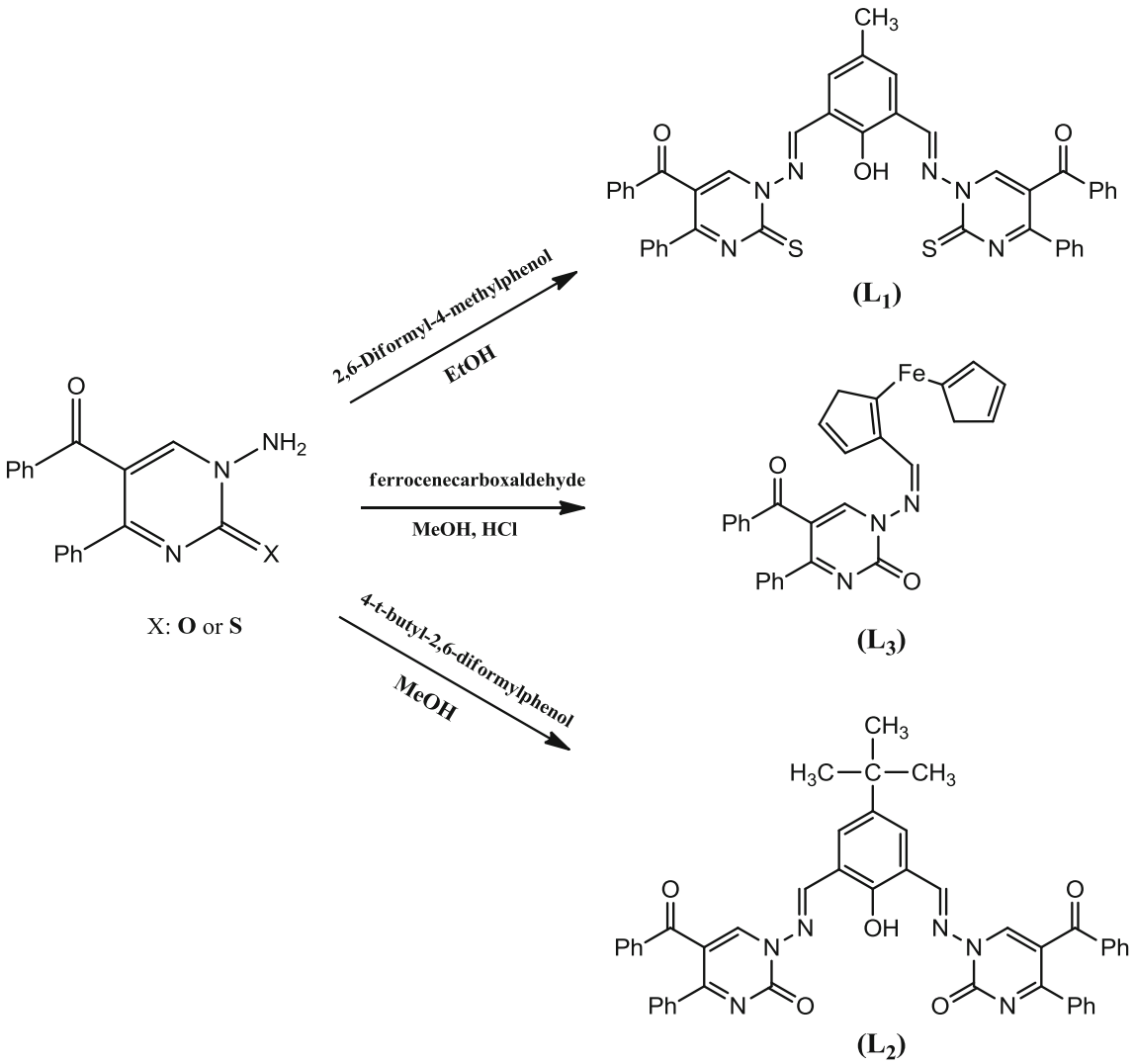

Fig. 1 Synthesis protocol of Schiff base ligands

The ^{1}H NMR and ^{13}C NMR spectra of the Schiff base ligand were carried out at room temperature in $CDCl_3$ and DMSO-d_6, respectively (Figs. 2 and 3).

The ^{1}H NMR spectrum of ferrocenyl Schiff base (L_3) showed the singlet at 8.99 ppm and 8.48 ppm were due to azomethine proton and pyrimidine ring (C–H) proton in the spectrum of the ligand, respectively. The multisignals corresponding aromatic protons appeared between at 7.80–7.33 ppm [23, 24]. The spectrum of ferrocenyl Schiff base exhibited cyclopentadienyl ring proton signals between at 4.40 and 4.84 ppm [25].

^{13}C NMR spectrum (Fig. 3) displayed characteristic signals at 192.1, 170.9 and 170.5 ppm due to the (OC-Ar), (C=O, pyrimidine) and (−C6, pyrimidine ring) of the L_3 ligand, respectively. The singlet peaks at 151.8 ppm was due to azomethine carbon of the ligand [24]. On the other hand, the spectrum of the ligand showed peaks in the region of 137.5–115.6 ppm, due to aromatic carbons. The observed signals between 75.2 and 69.7 ppm belongs to cyclopentadienyl ring carbons [26].

Fluorescence Features

The absorption and emission properties of the Schiff bases, L_1, L_2 and L_3 were studied at different solvents with different polarities of acetonitrile, methanol, ethanol, tetrahydrofuran and toluene and data obtained are presented in Table 1. The first absorption band of the compounds at λ_{max} between 304 and 418 nm may correspond to the π–π* transition of the azomethine group C=N while the second band between 383 and 576 nm may correspond to the n–π* transitions. As the polarity of the solvent is increased, while the absorption maxima of L_3 is red shifted, the absorption maxima of L_2 and L_1 are blue shifted, except for L_1 in toluene.

While the solvent polarity has nearly negligible effect on the emission maxima of the compounds, one interesting result is that only in ethanol the emission maxima of all the compounds is red shifted in comparison to all other solvents studied, presumably due to intramolecular proton transfer from the solvent to each derivative or hydrogen

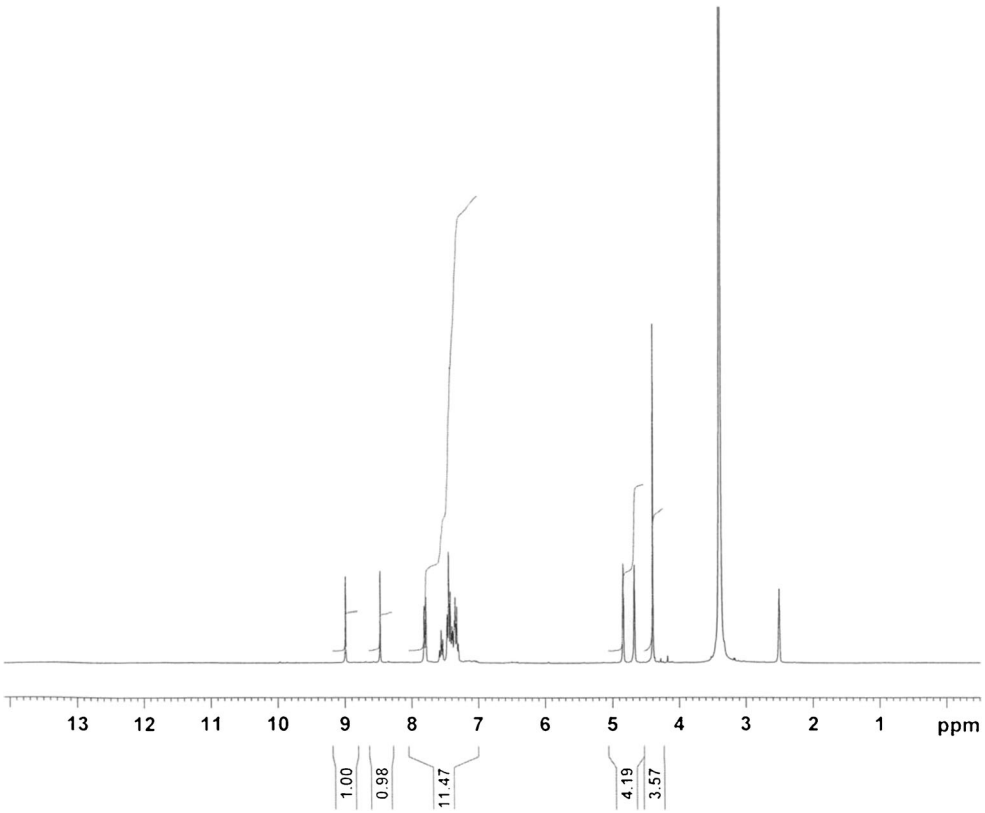

Fig. 2 ^{1}H NMR spectrum of L_3 Schiff base

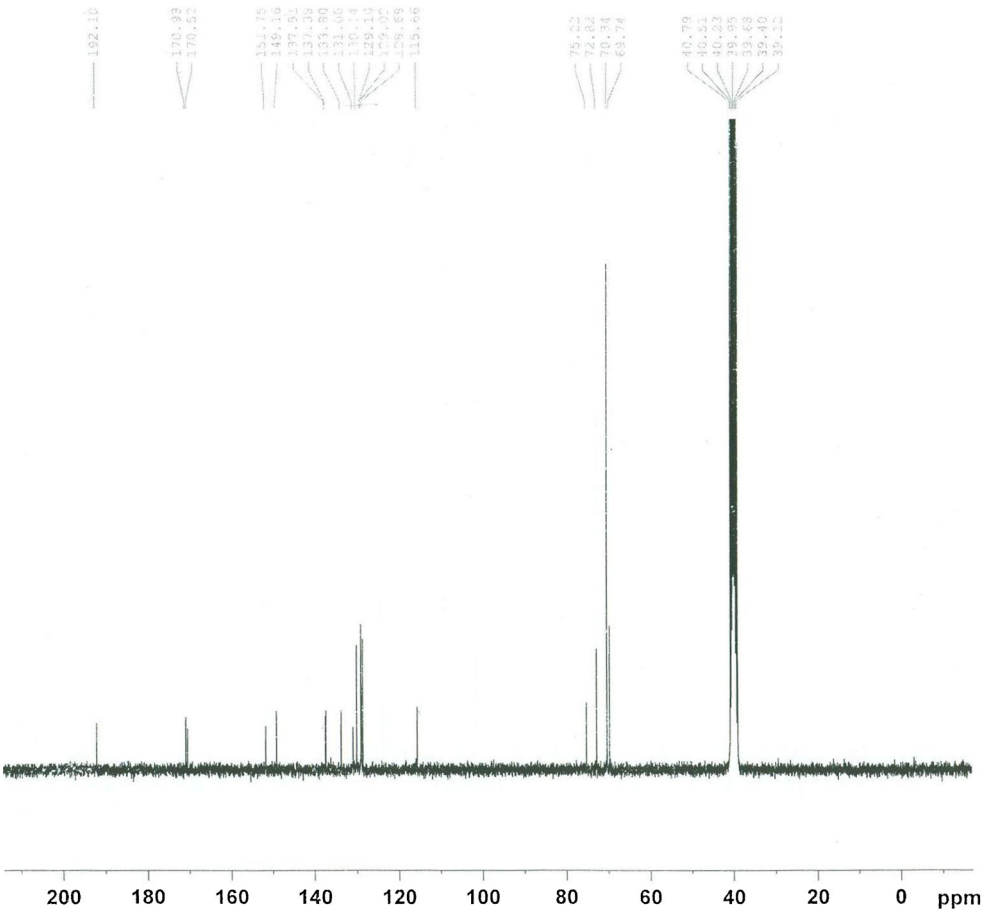

Fig. 3 ^{13}C NMR spectrum of L_3 Schiff base

Table 1 Adsorption and fluorescence emission data for compounds L_1, L_2 and L_3

Compound	Solvent	$\lambda^{abs}{}_{.max}{}^{1}$	$\lambda^{abs}{}_{.max}{}^{2}$	$\varepsilon_{max}{}^{1}$	$\varepsilon_{max}{}^{2}$	$\lambda^{emis.}{}_{Max}$	$\Delta\lambda$	Φ
L_3	Acetonitrile	346	460	3800	700	713	253	0,0132
	Methanol	346	478	50900	10100	715	237	0,0004
	Ethanol	348	480	3700	1800	731	251	0,0054
	Tetrahydrofuran	358	470	22600	5300	715	245	0,0013
	Toluene	360	470	2100	400	714	244	0,3732
L_2	Acetonitrile	348	468	8200	2700	655	187	0,0041
	Methanol	352	453	20000	7200	657	204	0,0144
	Ethanol	344	464	9200	1200	687	223	0,0312
	Tetrahydrofuran	342	475	5700	700	655	180	0,0247
	Toluene	304	383	43000	16400	656	273	0,0123
L_1	Acetonitrile	376	424	14900	7000	640	216	0,0040
	Methanol	348	440	41000	7900	639	199	0,0030
	Ethanol	352	464	9600	2700	736	272	0,0021
	Tetrahydrofuran	367	443	9700	1000	642	199	0,1920
	Toluene	418	576	14100	1900	640	64	0,0382

bonding. The longest wavelength emission maxima are observed for L_3 in the range of 714 and 731 nm, while L_2 and L_1 fluorescent nearly in the similar wavelength range, except for L_1 in ethanol (Fig. 4).

The compounds exhibited moderate Stokes' shift values ranging from 64 to 272 nm, which confers to the advantage of better spectral resolution in emission based studies.

The fluorescence quantum yields of compounds were determined by using Rhodammine 101 as a standard sample in ethanol. The highest quantum yield value was obtained for L_3 in tolune, for L_2 in ethanol and for L_1 in tetrahydrofuran (Table 1).

The photostability of the derivatives in dimethylformamide, acetonitrile, methanol, ethanol, tetrahydrofuran and toluene was determined with a steady-state spectrofluorimeter in time-based mode. The data were acquired at their maximum emission wavelengths. According to the data collected after 1 h, there was no change in the fluorescence intensities of the compounds (Fig. 5).

Electrochemical Analysis

The electrochemical properties of the present compounds were investigated by Cyclic voltammetric (CV) and on a glassy carbon electrode in dimethylformamide (DMF) containing 0.1 M tetrabutylammonium perchlorate (TBAP), in the concentration of 1×10^{-3} M vs. Ag/AgCl. The electrochemical data in peak potentials are reported in Table 2.

In the cathodic direction from +1.5 V to −2.3 V at scan rate of 100 mV s^{-1}, the CV of **L_1** is characterized by three cathodic waves (Ic, IIc and IIIc at about −1.84, −1.41 and −1.17 V, respectively) and anodic waves were not observed as depicted by CV given in Fig. 6a. These peaks were irreversible. At higher scan rates (> 100 mV s^{-1}) the oxidation process peaks became more intense (Fig. 7a).

The electrochemical behavior of the **L_2** is presented in Fig. 6b. In the CV measurements upon scanning cathodically at the negative potential side (from +1.5 to −2.3 V at 100 mV s^{-1}), the CV of **L_2** is characterized by one cathodic

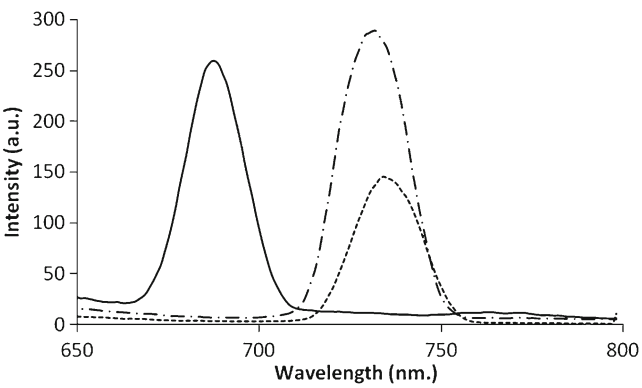

Fig. 4 Fluorescence spectra of L_1 (····), L_2 (–) and L_3 (– · –) compounds in ethanol

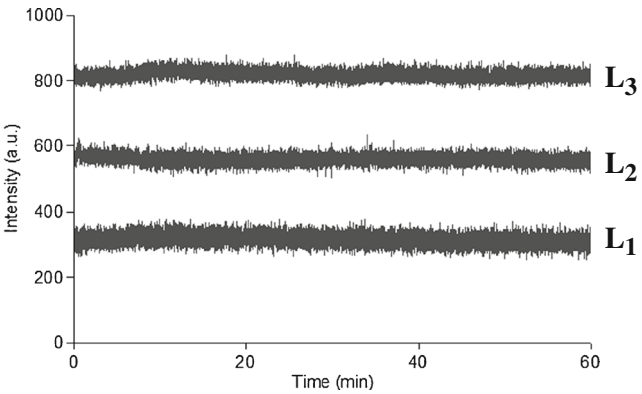

Fig. 5 Photostability test results of L_1, L_2 and L_3 in tetrahydrofuran after 1 h of monitoring

Table 2 Voltammetric results at scan rate of 100 mVs^{-1} vs. Ag/AgCl. Ec: cathodic potential, Ea: anodic potential

Compound	*Ec*	*Ea*
$\mathbf{L_1}$	**Ic:**-1.84, **IIc:**-1.41, **IIIc:**-1.17	
$\mathbf{L_2}$	**Ic:**-1.99, **IIc:**-1.65, **IIIc:**-0.65, **IVc:**-030	**Ia′:**+0.74 **IIIa:**-0.40
$\mathbf{L_3}$	**Ic:**-1.36, **IIc:**-1.62, **IIIc:**-2.05	**Ia′**:+1.42

peak (Ic at about −1.99 V) and one anodic wave (Ia' at about +0.74 V) (Fig. 6b). At higher scan rates (≥ 200 mV s^{-1}) three new cathodic waves were located at about −1.65, −0.65 and −0.30 V (IIc, IIIc and IVc, respectively) and a new anodic peak was observed at about IIIa (at *ca*. −0.40 V) (Fig. 7b). ΔE_p for IIIa/IIIc from this redox couple was also found to be 250 mV. This is a indication of a quasi-reversible electron transfer in the electrode reaction.

The voltammograms of $\mathbf{L_3}$ compound were investigated under the same experimental conditions (from + 1.5 V to −2.3 V at 100 mVs^{-1} in Fig. 6c), three cathodic waves (Ic, IIc, and IIIc at about −1.36, −1.62 and −2.05 V, respectively) and one anodic wave (Ia' at about +1.42 V). At higher scan rates (≥ 200 mVs^{-1}) the oxidation process Ia became more intense (Fig. 7c). However, at higher scan rates (≥ 400 mVs^{-1}) the IIIc peak wasn't observed (Fig. 7c).

It was found that the initial oxidation peak current of $\mathbf{L_1}$, $\mathbf{L_2}$ and $\mathbf{L_3}$ gradually increased and a negative shift in the peak potential existed with increasing scan rate by using the CVs (Fig. 7). A plot of logarithm of peak current significantly correlated with the logarithm of scan rate for all $\mathbf{L_1}$, $\mathbf{L_2}$ and $\mathbf{L_3}$ with slopes between 0.45, 0,48 and 0.52, respectively (correlation coefficient between 0.987, 0.976 and 0.991). by using the CV results obtained between 10 and 1,000 mVs^{-1}. These results showed that the redox processes were predominantly diffusion controlled in the whole scan rate range studied.

Taking into account the reported data concerning electrochemical behavior of recently synthesized pyrimidine compounds such as 1-amino-5-benzoyl-4 phenyl-1H-pyrimidine-2-one [27] and 2-iminopyrimidines or 2-thioxopyrimidine [28], N-(5-benzoyl-2-oxo-4-phenyl-2H-pyrimidin-1-yl)-oxalamic acid or malonamic acid [29, 30] at hanging mercury drop and glassy carbon electrodes, respectively, the electron-donating groups lowered the oxidation potentials, while electron-withdrawing groups had the opposite effect [31] There was a mechanism involving self-protonation reactions in the electrochemical reduction of the imine or thio, and carbonyl groups in pyrimidines in the 2-iminopyrimidines and 2-thioxopyrimidine [28].

Functional groups of (C=S) and/or (C=O) are probably reduced in the compounds. In all these compounds, the common functional group is imin (C=N) group. If reduction was over imin (C=N) group which is common in all compounds, there would not be a distinctive difference among reduction potentials of three compounds. However, we think the fact that L_1 has more positive reduction potential can only be explained this way. Furthermore, $\mathbf{L_1}$, $\mathbf{L_2}$ and $\mathbf{L_3}$ compounds have the same functional groups. However, since $\mathbf{L_1}$ has (C=S) functional group, in which the sulfur atom is a softer as a difference from

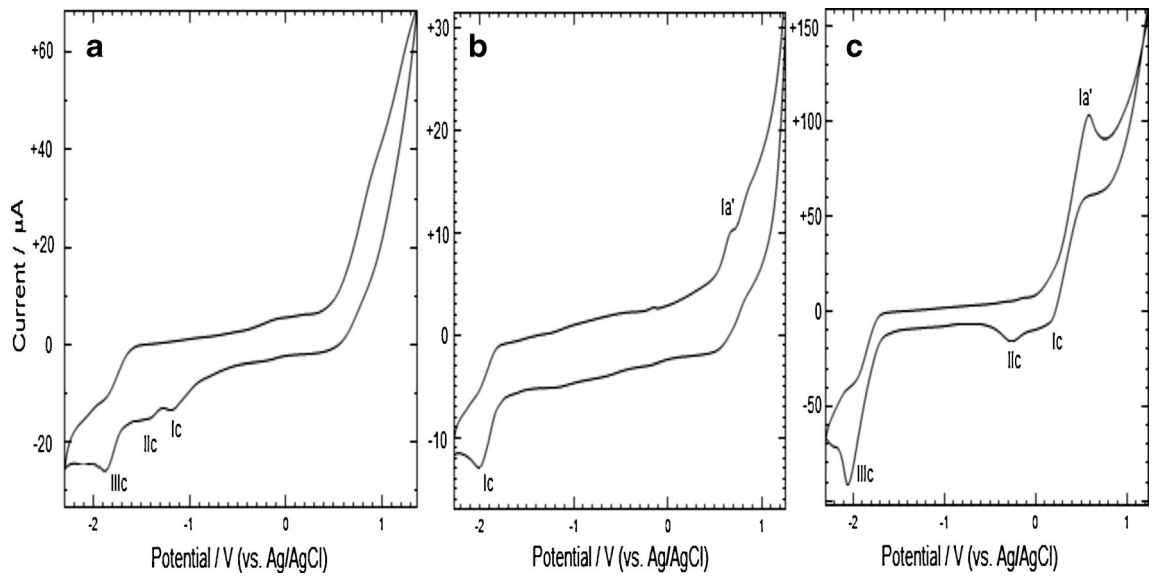

Fig. 6 Cyclic voltammogram of A ($\mathbf{L_1}$), B ($\mathbf{L_2}$) and C ($\mathbf{L_3}$) compounds (1×10^{-3} M) at 100 mVs^{-1} scan rate on glassy carbon electrode in DMF/TBAP

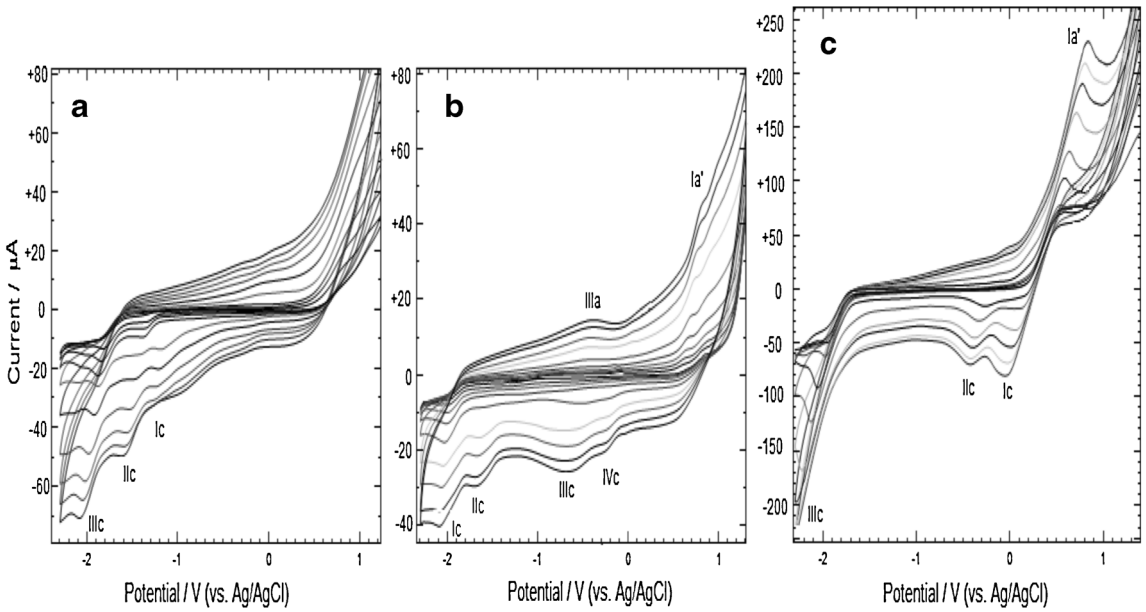

Fig. 7 Cyclic voltammograms of A ($\mathbf{L_1}$), B ($\mathbf{L_2}$) and C ($\mathbf{L_3}$) compounds (1×10^{-3} M) at on glassy carbon electrode in DMF/TBAP at various scan rates (10, 25, 50, 100, 200, 400, 600, 800 and 1,000 mVs^{-1})

the others, its reduction potential is more positive than the others.

Experimental

Reagents and General Techniques

All chemicals are commercially available and were used without further purification. All reagents and solvents were of reagent grade quality and were obtained from commercial suppliers. All solvents were dried by refluxing with appropriate drying agents and distilled before use. The homogeneity of the products was tested in each step by TLC (SiO_2). Ferrocenecarboxaldehyde, 4-*t*-butyl-2,6-diformylphenol were purchased from Aldrich Chem. Co. 1-Amino-5-benzoyl-4-phenyl-1*H*-pyrimidine-2-thione, 1-Amino-5-benzoyl-4-phenyl-1*H*-pyrimidine-2-one [32] and 2,6-diformyl-4-methylphenol [33] were synthesized according to the method described in literature.

The elemental analyses (C, H, N, S) were performed by using Leco CHNS model 932 elemental analyzer. FT-IR spectra were obtained using KBr pellets (4,000–400 cm^{-1}) on Bio-Rad-Win-IR Spectrophotometer. The ^1H NMR and ^{13}C NMR spectra of the Schiff bases were taken on a Bruker 300 MHz Ultrashield TM NMR instrument. UV/visible absorption spectra were recorded with Schimadzu UV-1601 spectrophotometer (Tokyo, Japan). All fluorescence measurements were undertaken by using Varian-Carry Eclipse spectrofluorimeter (Mulgrave, Australia).

Synthesis of Schiff Base Ligands

2,6-bis((E)-((5-Benzoyl-2-oxo-4-Phenylpyrimidin-1(2H)-yl) Imino)Methyl)-4-(Methyl)Phenol (L_1)

Synthesis and structural characterisations were described previously [34].

2,6-bis((E)-((5-Benzoyl-2-oxo-4-Phenylpyrimidin-1(2H)-yl) Imino)Methyl)-4-(Tert-Butyl)Phenol (L_2)

Synthesis and structural characterisations were described previously [35].

(2-(((5-Benzoyl-2-oxo-4-Phenylpyrimidin-1(2H)-yl)Imino) Methyl)Cyclopenta-1,3-Dien-1-yl)(Cyclopenta-1,3-Dien-1-yl) Iron (L_3)

The Schiff base ligand (L_3) was prepared by 1:1 condensation reaction between N-aminopyrimidine-2-one and ferrocenecarboxaldehyde. Ferrocenecarboxaldehyde (0.214 g, 1 mmol), N-aminopyrimidine-2-one (0.291 g, 1 mmol) and hot methanol solution (30 mL) containing few drops of HCl were mixed slowly with a constant stirring (Fig. 1). Then the mixture was refluxed for 2 h. A red precipitate was formed. The isolated solid precipitate was filtered off, washed with hot methanol and diethylether and then dried in vacuum over P_2O_5. Claret red, yield was 380 mg (78 %), Mp 215 °C. Anal. Calc. for $C_{28}H_{21}FeN_3O_2$ (487,33 g/mol): C, 69.01; H, 4.34; N, 8.62. Found: C, 68.77; H, 4.24; N, 8.53 %. Selected IR data (KBr, ν cm^{-1}): 3064 $\nu(C–H_{pyrimidine})$, 1643 $\nu(C=O)$, 1599 $\nu(C=N_{azomethine})$. ^1H NMR (300 MHz, $CDCl_3$): δ=8.99 (s, 1H),

8.48 (s, 1H), 7.80 (d, J=7.4 Hz 2H, ArH), 7.54 (t, J=7.4 Hz, 1H, ArH), 7.45 (t, J=6.6 Hz, 2H, ArH), 7.40–7.33 (m, 5H, ArH), 4.84 (quasitriplet, J=1.7 Hz, 2H, FerroceneH), 4.68 (quasitriplet, J=1.7 Hz, 2H, FerroceneH), 4.40 (bs, 5H, FerroceneH) ppm. ^{13}C NMR (75 MHz, DMSO-d_6): δ =192.1, 170.9, 170.5, 151.8, 149.2, 137.5, 137.4, 133.8, 131.0, 130.1, 129.1, 129.0, 128.7, 115.7, 75.2, 72.8, 70.3, 69.7 ppm.

Electrochemical Assay

Electrochemical experiments were performed with an Autolab PGSTAT 128 N potentiostat, (The Netherlands) using a three electrode system, glassy carbon as a working electrode (Φ: 3 mm, BAS), platinum wire as an auxiliary electrode and Ag/AgCl (NaCl 3 M, Model RE-1, BAS, USA) as a reference electrode. The reference electrode was separated from the bulk solution by a fritted-glass bridge filled with the solvent/supporting electrolyte mixture. Before starting each experiment, the glassy carbon electrode was polished manually with alumina (Φ: 0.01 μm). CV experiments were recorded at room temperature in extra pure DMF, and ionic strength was maintained at 0.1 mol L^{-1} with electrochemical grade TBAP as the supporting electrolyte. Solutions were deoxygenated by a stream of high purity nitrogen for 10 min prior to the experiments, and during the experiments nitrogen flow was maintained over the solution.

Acknowledgments The authors wish to thank Presidency of Scientific Research Projects of University of Yuzuncu Yil (2011-FED-B009) for the financial support.

References

1. Taha ZA, Ajlouni AM, Al-Hassan KA, Hijazi AK, Faig AB (2011) Syntheses, characterization, biological activity and fluorescence properties of bis-(salicylaldehyde)-1,3-propylenediimine Schiff base ligand and its lanthanide complexes. Spectrochim Acta A 81:317–323
2. Zhou L, Cai P, Feng Y, Cheng J, Xiang H, Liu J (2012) Synthesis and photophysical properties of water-soluble sulfonato-Salen-type Schiff bases and their applications of fluorescence sensors for Cu2+ in water and living cells. Anal Chim Acta 735:96–106
3. Guo D, Wu P, Tan H, Xia L, Zhou W (2011) Synthesis and luminescence properties of novel 4-(N-carbazole methyl) benzoyl hydrazone Schiff bases. J Lumin 131:1272–1276
4. Majumder A, Rosair GM, Mallick A, Chattopadhyay N, Mitra S (2006) Synthesis, structures and fluorescence of nickel, zinc and cadmium complexes with the N, N, O-tridentate Schiff base N-2-pyridylmethylidene-2-hydroxy-phenylamine. Polyhedron 25: 1753–1762
5. Basak S, Sen S, Marschner C, Baumgartner J, Batten SR, Turner DR, Mitra S (2008) Synthesis, crystal structures and fluorescence properties of two new di- and polynuclear Cd(II) complexes with N2O donor set of a tridentate Schiff-base ligand. Polyhedron 27: 1193–1200
6. Cleiton M, Da S, Daniel L, da S, Luzia V, Modolo RBA, Maria A, de R, Cleide VB, Martins A d F (2011) Schiff bases: a short review of their antimicrobial activities. J Adv Res 2:1–8
7. Khuhawar MY, Mughal MA, Channar AH (2004) Synthesis and characterization of some new Schiff base polymers. Eur Polymer J 40:805–809
8. Pandeya SN, Srirama D, Nathb G, DeClercq E (1999) Synthesis, antibacterial, antifungal and anti-HIV activities of Schiff and Mannich bases derived from isatin derivatives and N-[4-(4′-chlorophenyl)thiazol-2-yl] thiosemicarbazide. Eur J Pharma Sci 9:25–31
9. Muratov N, Mescheriakov AK (2005) Investigation of anticancer activity of macrocyclic Schiff bases by means of 4D-QSAR based on simplex representation of molecular structure. SAR QSAR Environ Res 16:219–230
10. Casellato U, Vigato PA (1977) Transition metal complexes with binucleating ligands. Coord Chem Rev 23:31–50
11. Kandil SS, Katib SMA, Yarkandi NHM (2007) Nickel(II), Palladium(II) and Platinum(II) Complexes of *N′*-Allyl-*N′*-pyrimidin-2-ylthiourea. Trans Met Chem 32:791–798
12. Fahmy HTY, Sherif Rostom SAF, Bekhit AA (2002) Synthesis and antitumor evaluation of new polysubstituted thiazole and derived thiazolo[4,5-d] pyrimidine systems. Arch Pharm Pharm Med Chem 5:213–222
13. Nasr MN, Gineinah MM (2002) Pyrido[2,3-d]pyrimidines and pyrimido[50,40:5,6]pyrido [2,3-d]pyrimidines as new antiviral agents: Synthesis and biological activity. Arch Pharm 335:289–295
14. Tozkoparan B, Ertan M, Kelicen P, Demirdamar R (1999) Synthesis and anti-inflammatory activities of some thiazolo[3,2-a]pyrimidine derivatives. Il Farmaco 54:588–593
15. Amr EA, Ashraf MM, Salwa FM, Nagla AA, Hammam AG (2006) Anticancer activities of some newly synthesized pyridine, pyrane, and pyrimidine derivatives. Bioorg Med Chem 14:5481–5488
16. Kumar N, Singh G, Yadav AK (2001) Synthesis of some new pyrido_2,3-d_pyrimidines and their ribofuranosides as possible antimicrobial agents. Heteroat Chem 12:52–56
17. Mangalagiu G, Ungureanu M, Grosu G, Mangalagiu I, Petrovanu M (2001) New pyrrolo-pyrimidine derivatives with antifungal or antibacterial properties. Ann Pharm Fr 59:139–140
18. Viciano-Chumillas M, Tanase S, Aromí G, Smits JMM, de Gelder R, Solans X, Bouwman E, Reedijk J (2007) Coordination Versatility of 5(3)-(2-Hydroxyphenyl)-3(5)-methylpyrazole: Synthesis, Crystal Structure and Properties of Co^{III}, Ni^{II} and Cu^{II} Complexes. Eur J Inorg Chem 18:2635–2640
19. Roy S, Mandal TN, Barik AK, Pal S, Gupta S, Hazra A, Butcher RJ, Hunter AD, Zeller M, Kar SK (2007) Metal complexes of pyrimidine derived ligands—Syntheses, characterization and X-ray crystal structures of Ni(II), Co(III) and Fe(III) complexes of Schiff base ligands derived from *S*-methyl/*S*-benzyl dithiocarbazate and 2-*S*-methylmercapto-6-methylpyrimidine-4 carbaldehyde. Polyhedron 26:2603–2611
20. Salih NA (2008) Synthesis and characterization of novel azole heterocycles based on 2,5-disubstituted thiadiazole. Turk J Chem 32:229–235
21. Roy S, Westmaas JA, Buda F, Reedijk J (2009) Platinum(II) compounds with chelating ligands based on pyridine and pyrimidine: DNA and protein binding studies. J Inorg Biochem 103: 1288–1297
22. Nakamoto K (1997) Infrared spectra and Raman spectra of inorganic and coordination compounds. John Wiley & Sons, New York
23. Tümer M, Deligönül N, Gölcü A, Akgün E, Dolaz M, Demirelli H, Dığrak M (2006) Mixed-ligand copper(II) complexes: investigation of their spectroscopic, catalysis, antimicrobial and potentiometric properties. Trans Met Chem 31:1–12
24. Sönmez M, Çelebi M, Berber İ (2010) Synthesis, spectroscopic and biological studies on the new symmetric Schiff base derived

from 2,6-diformyl-4-methylphenol with N-aminopyrimidine. Eur J Med Chem 45:1935–1940
25. Huang G, Song Q, Ma Y (2001) Metal complexes of ferrocene-carboxaldehyde 2,4 dichlorobenzoylhydrazone. Synth React Inorg Met Org Chem 31:297–302
26. Pal SK, Krishnan A, Das PK, Samuelson AG (2000) Schiff base linked ferrocenyl complexes for second-order nonlinear optics. J Organomet Chem 604:248–259
27. Kılıç H, Berkem M (2004) Electrochemical behavior of some new pyrimidine derivatives. J Serb Chem Soc 69:689–703
28. Akbas E, Levent A, Gümüş S, Sümer MR, Akyazı İ (2010) Synthesis of some novel pyrimidine derivatives and investigation of their electrochemical behavior. Bull Korean Chem Soc 31:3632–3638
29. Sönmez M, Çelebi M, Levent A, Berber İ, Şentürk Z (2010) Synthesis, characterization, cyclic voltammetry, and antimicrobial properties of *N*-(5-benzoyl 2-oxo-4-phenyl-2*H*-pyrimidine-1-yl)-malonamic acid and its metal complexes. J Coord Chem 63:1986–2001
30. Sönmez M, Çelebi M, Levent A, Berber İ, Şentürk Z (2010) A new pyrimidine-derived ligand, *N*-pyrimidine oxalamic acid, and its Cu(II), Co(II), Mn(II), Ni(II), Zn(II), Cd(II), and Pd(II) complexes: synthesis, characterization, electrochemical properties, and biological activity. J Coord Chem 63:848–860
31. Cai T, Xian M, Wang PG (2002) Electrochemical and peroxidase oxidation study of *N′*-Hydroxyguanidine derivatives as NO donors. Bioorg Med Chem Lett 12:1507–1510
32. Akçamur Y, Altural B, Sarıpınar E, Kollenz G, Kappe O, Peters K, Peters E, Schering HJ (1988) A convenient synthesis of functionalized 1*H*-pyrimidine-2-thiones. Heterocycl Chem 25:1419–1422
33. Gagne RR, Spiro CL, Smith TJ, Hamann CA, Thies WR (1981) Shiemke; A.K. The synthesis, redox properties, and ligand binding of heterobinuclear transition-metal macrocyclic ligand complexes. Measurement of an apparent delocalization energy in a mixed-valent copper(I)copper(II) complex. J Am Chem Soc 103: 4073–4081
34. Gülcan M., İspir E, Sönmez M (2012) International Symposium on Metal Complexes, vol. 2. Lisbon, Portugal.
35. Gülcan M, Çelebi M, Sönmez M (2012) International Symposium on Metal Complexes, vol. 2. Lisbon, Portugal.